Journal of Sustainable Construction Materials and Technologies
Web page info: https://jscmt.yildiz.edu.tr
DOI: 10.14744/jscmt.2021.01

JSCMT

Journal of Sustainable Construction
Materials and Technologies

Original Article

Plaster of Paris containing zero valent iron particles: Designing a permeable reactive barrier, used for remediation of 4-nitroaniline pollution

Saliha BOUDIA[1,2] , **Farida FERNANE**[1] , **Patrick SHARROCK**[2,3] , **Marina FIALLO**[2*]

¹Mouloud Mammeri University, Natural Resources Laboratory, Tizi-Ouzou, Algeria
²Chemistry department, Université Toulouse 3 Paul Sabatier, Castres, France
³RAPSODEE, Ecole des Mines, Albi, France

ABSTRACT

Permeable reactive barrier (PRB) containing zero valent iron (ZVI), plaster and additives to make a porous composite structure, was tested to remove an organic nitro compound as model pollutant. An aqueous solution of 4-nitroaniline (PNA) was passed through a porous plaster column and chemical degradation quantified by UV-Vis spectroscopy. PNA was reduced to p-phenylenediamine and the rate of the reduction was strongly related to ZVI amount, pollutant volume, and the contact rate with the metal particles. The PBR could be controlled by design and operation. Test columns were made to evaluate the materials for making precast plaster blocks containing ZVI. The results showed that such porous plaster blocks could be efficient as retaining funneling walls for environmental applications. Thus economical Calcium sulphate solids can be used for making remediation columns for depolution with reactive products such as iron metal with capacity for treating unwanted toxic nitrates, or chlorinated-solvents present in waterways. A reactive permeable barrier containing zero valent iron will last as long as some iron particles remain to react.

Cite this article as: Boudia S, Fernane F, Sharrock P, Fiallo M. Plaster of Paris containing zero valent iron particles: Designing a permeable reactive barrier, used for remediation of 4-nitroaniline pollution. J Sustain Const Mater Technol 2021;6:4:124–134.

1. INTRODUCTION

Permeable reactive barrier (PRB) is a cost-effective technology for groundwater remediation [1]. It is an implementation of filtration consisting in porous material, which passively captures a plume of contaminants through immobilization or transformation of pollutants, releasing decontaminated water to the other side of the barrier [2]. PRB is generally composed of inexpensive filler materials, doped with specific reagents for remediation of unwanted compounds. It was reported that zero valent iron (ZVI) is particularly effective in chemical degradation of persistent chlorinated compounds into non-toxic and harmless by-products [3–5].

Nitroarenes can be reduced to corresponding anilines, in presence of ZVI, in Bechamp reduction [6]; moreover, in organic synthesis other methods were found to be more specific and to reduce by-pass products [7]. For instance,

---

*****Corresponding author.**
*E-mail address: marina.fiallo@iut-tlse3.fr

silver nanoparticles were developed for in situ catalytic reduction method of PNA [8]. However, in order to be integrated in a PRB low cost reactant, ZVI has already shown to be a good candidate for reduction of different pollutants [9–11]. Efficiency of a PRB is related to the nature and flow of polluted plume [12, 13].

Calcium sulfates (plaster, $CaSO_4.0.5H_2O$, and its dihydrated product, gypsum, $CaSO_4.2H_2O$) were chosen as "inert substrate" in order to prepare porous composites. They are low cost building materials, sometime considered as a waste when containing phosphogypsum [14, 15]. We researched the possibility of using plaster for making PRB with ZVI as a low cost reactive component. Our aim was to verify if ZVI retains its redox properties when included in a solid shell, shaped as a column and with 4-nitroanilineas pollutant model.

Key factors for all-in-one design of composites for PRB were investigated as follows: permeability of solid plaster, as inert support for PRB, was determined and improved (giving "porous" plaster). "Porous" plaster was tested for its mechanical properties and the best formulas chosen. ZVI was inserted in "porous" plaster and new composites were optimized for all parameters. Reduction of 4-nitroaniline was performed batchwise with ZVI and its degradation to p-phenylenediamine (PDA), was quantified by UV spectroscopy. Reduction of 4-nitroaniline was performed in a downflow column: breakdown and exhaustion points were determined for specific experimental conditions.

2. MATERIALS AND METHODS

2.1. Chemicals

Plaster, in chemical form of $CaSO_4.0.5H_2O$, was a commercial powder (plaster of Paris quality) from Parexlanko, France; iron powder (ZVI, 325 mesh, 99%), H_3PO_4 (85%), and $CaCO_3$ (99%) were from Acros (France), 4-nitroaniline (p-nitroaniline, PNA, 98%), p-phenylendiamine (PDA, 98%), o-phenanthroline (98%) and KSCN (97%) from Aldrich (France).

2.2. Plaster Samples Preparation

Plaster slabs were made by adding plaster powder (50 g) to appropriate amounts of distilled water. After 5 minutes of mixing, preparations were poured into PET (polyethylene terephtalate) or PE (polyethylene) cylindrical molds to make samples for flow experiments (in 2.8-cm- diameter, 2-cm-high) and for mechanical tests and density measurements (in 2.6-cm-diameter, 5-cm-heigh). All solid samples were dried at 60°C for 24 hours before their use. All samples were weighted and "apparent" density calculated from geometrical parameters.

2.3. Material Characterization
2.3.1. XRD and SEM Analysis

Solid samples were characterized by powder X-ray diffraction (XRD) with a Bruker D2 X'PertPRO diffractometer using Cu Kα radiation (40 kV and 40 mA). Crystallographic identification of $CaSO_4.2H_2O$ was accomplished by comparing the experimental XRD pattern to COD 2300259 of gypsum standard (point group 2/m). Plaster samples were observed by scanning electron microscopy (SEM) Zeiss Supra 55VP.

2.3.2. Mechanical Tests

Indirect tensile stress diametral compression tests were carried out with a Zwick Roll Z020 testing machine (Zwick Roell, France) at a cross-head speed of 10 mm/min, until failure. Using initial height (L [m]) and diameter (D [m]) of each sample, and measuring the reciprocated force (F [kg m/s²]) from compression, indirect (or Brazilian) tensile strength, σ_T ([kg/m s²]), was calculated from its definition in equation 1:

$$\sigma_T = 2F/(\pi LD) \tag{1}$$

2.3.3. Porosity Determination

Porosity was determined from the ratio of experimental "apparent" density of each sample and gypsum density, $CaSO_4.2H_2O$, 2.308 g/cm³ [16] with equation 2:

$$porosity\ (\%) = (density_{exp}/density_{gypsum}) * 100 \tag{2}$$

2.3.4. Permeability Coefficient Measurements

Permeability coefficient measurements were done on plaster samples (2.8-cm diameter, 2.0-cm heigth) with a water pressure column of 5 cm. Discharge of water (Q [m³/s]), percolating under a constant head difference (H [m]) through a sample of porous material of cross area S ([m²]) and length L ([m]), was determined for several samples. Permeability coefficients K (hydraulic conductivity, [m/s]) were calculated from Darcy's law, following equation 3:

$$K = (QL)/(SH) \tag{3}$$

2.4. Bechamp Reduction
2.4.1. Spectroscopic Analysis

Vis-UV spectra were used to quantify 4-nitroaniline (PNA) and p-phenylendiamine (PDA) concentrations. They were recorded between 200 and 700 nm in aqueous solution on a HP 8453 spectrophotometer with quartz cells of 0.2 and 1 cm of path-length. Spectra of pure 4-nitroaniline (PNA) and p-phenylendiamine (PDA) were recorded in aqueous solution giving the following spectroscopic features: PNA: 380 (ε=73.3 l mol⁻¹cm⁻¹), 227 (35.5), 204 (63.0) nm. PDA: 305 (ε=13.7 l mol⁻¹cm⁻¹), 240 (49.3), 210 (58.7) nm. PNA concentrations in solution were determined by measuring absorbance at 380 nm. PDA formation (in Bechamp reduction) was checked from band at 240 nm (PDA maximum absorption).

2.4.2. Determination of PNA Degradation

Degradation of PNA, meaning the disappearing of its characteristic absorption band at 380 nm, was calculated from the UV-Vis spectra (Fig. S1) with equation 4:

$$degradation \ (\%)=(A_{380}-A_{600})/(A°_{380}-A°_{600})*100 \qquad (4)$$

where A_{380} and A_{600} are the absorption values of each sample at the noted wavelengths, and $A°_{380}$ and $A°_{700}$ the absorption values of starting solutions. Absorption values were corrected at 600 nm in order to avoid diffusion effects from cloudy solutions. At 380 nm the absorption contribution for presence of PDA in aqueous solutions was insignificant.

2.4.3. ZVI in Batch

Batch experiments were conducted inside 250 ml Erlemeyer flasks under continuous magnetic stirring (500 rpm) and the overall time of experiments was 7 hours. Batch experimental initial conditions were: temperature; 25°C, PNA concentration; 30 mg/l, water volume; 100 ml. Specific variables in batch experiments included pH (initial pH acidic or neutral) and the amounts of ZVI (1, 2 and 3 g). Sampling was conducted within accumulative time of 15 minutes during first three hours, then of 1 hour for last four in batch experiments. For analysis, 2 ml samples were withdrawn by a 5 ml syringe, their Vis-UV spectra registered using a 1 cm quartz cell, then returned to batch. Initial pH was adjusted, or not, using 95% phosphoric acid. Degradation percentage was calculated from absorbance values at 380 nm.

2.4.4. Column Preparation

100 g of plaster, mixed with appropriate amounts of ZVI and 0.2% $CaCO_3$, were added to 70 ml of distilled water, containing 0.4 g of phosphoric acid, then all reagents were mixed together and the viscous mixture poured into PET (polyethylene terephtalate) cylindrical molds (in 5.0-cm-diameter, 15-cm-heigh) used as percolator system. PET shells were thermally fixed to plaster columns in order to avoid leaking from their extremities.

2.4.5. ZVI in Column

PNA-containing aqueous solutions (100 ml aliquots) were passed by percolation through columns. Fractions of 100 ml were recovered post-column: 2 ml of each fraction were checked by UV-Vis spectrum between 200 and 700 nm and absorbance values at 380 nm for used to calculate PNA concentration in each fraction.

2.4.6. Identification of Ionic Species

Samples of plaster-based composites (2.8-cm diameter, 2.0-cm heigth) were soaked in distilled water (25 ml) and pH was measured as a function of time. KSCN (1%) and o-phenanthroline (0.5%) in aqueous solution were used to check by colorimetry presence of Fe(II) or Fe(III) species, respectively.

3. Results and Discussion

Hemihydrate calcium sulphate ($CaSO_4.0.5H_2O$), named plaster, became gypsum when hydrated ($CaSO_4. 2H_2O$). Different formulations prepared, by using plaster, water, chemical porogen ($CaCO_3$) and ZVI in different proportions, were realized as expected. For each sample, density, porosity, permeability, and mechanical properties were determined in straightforward fashion. Figure 1 indicated effects of plaster slab chemical composition on mechanical properties and porosity. Detailed values, as well as densities as a function of chemical composition, were reported in Tables A.1, A.2 and A.3.

3.1. Properties of Plaster-Based Composites
3.1.1. Effect of Water

Water/plaster ratio was modified, and physical and mechanical properties were measured for each sample (Fig. 1a, Table A.1). It was reported that water amount determined porosity in plasters blocks [17, 18]; as reported in Figure 1a, indirect tensile strength of plaster was reduced as a function of water content whereas porosity increased. During reaction between plaster ($CaSO_4.0.5H_2O$) and water to form gypsum ($CaSO_4.2H_2O$), part of water was consumed by hydration reaction during material setting and remainder slowly evaporated leading to porosity [19]; hardening of plaster paste lead to porous structure, made of entangled needle-shape gypsum crystals [20].

3.1.2. Effect of Porogen ($CaCO_3+H_3PO_4$)

Porous samples were prepared by adding fine calcium carbonate with plaster powder, then pouring the powder in phosphoric acid–containing aqueous solution. Calcium carbonate was used as porogen in presence of acid in order to generate open porosity and increase permeability through the column (Fig. 1b); phosphoric acid was chosen because formation of calcium phosphate as secondary product gave composites with enhanced mechanical properties and lower dissolution rates [21].

In presence of increasing amount of H_3PO_4, porosity increased while density and mechanical properties decreased. These results are in agreement with cavity formation following CO_2 evolution during material setting (Table A.2). Starting from 0.5% acid, porosity was not significantly modified, as well as mechanical properties. However, permeability increased three times in magnitude compared to "compact" plaster. Calcium phosphate, formed by reaction of phosphoric acid with calcium carbonate [22], was dispersed in gypsum matrix with no effects on physical and mechanical parameters. It was reported that weak acids (such as citric acid) play a role as plastifier, retarding setting [23]. In fact, citric acid partially inhibits binder hydration from hemihydrate to dihydrate. Total porosity seemed little affected by increasing the amount of $CaCO_3$, pore dimensions were bigger (Fig. 2) and SEM images of porogen-containing samples showed 1 mm pores.
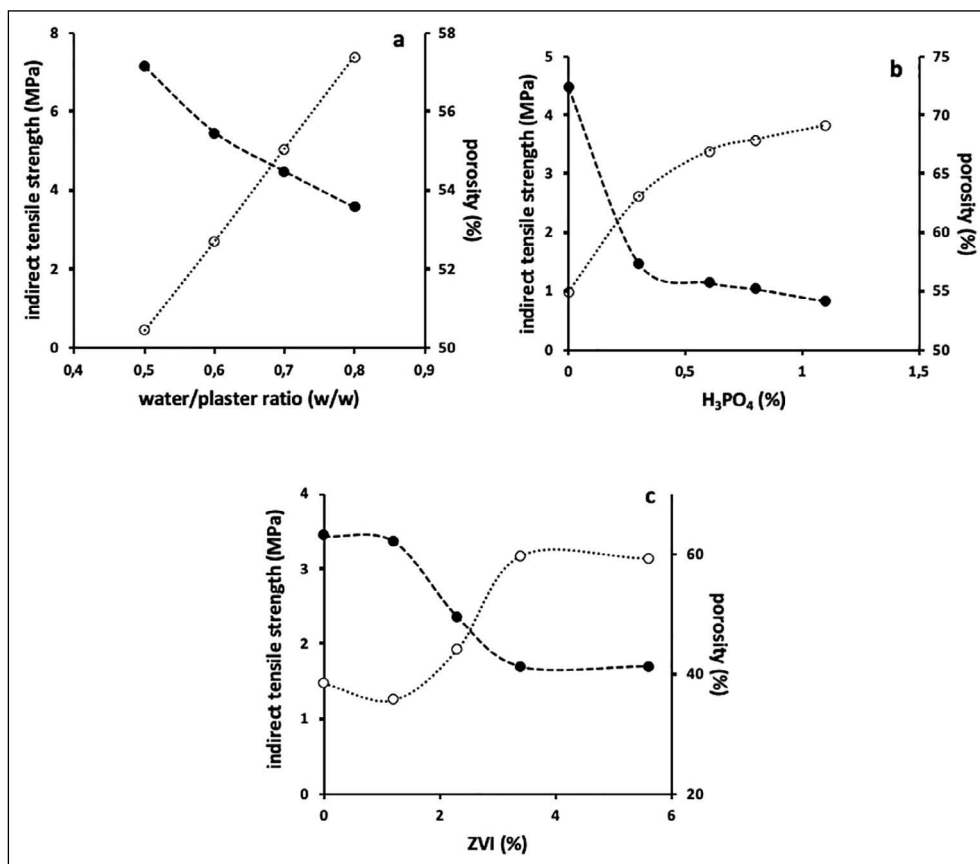
Figure 1. **(a)** Indirect tensile strength (closed signet) and porosity (empty signet) as a function of plaster composition as a function of: **(b)** water, (b) H_3PO_4, **(c)** ZVI amounts; experimental conditions: plaster (50.0 g).

3.1.3. Effect of ZVI

Different amounts of ZVI were dispersed in solid components (plaster and calcium carbonate) before adding water and phosphoric acid, in order to uniformly scatter the heavier iron particles in the slab. Physical and mechanical properties of different samples obtained were reported in Fig. 1c. Depending on ZVI amounts (Table A.3), density and mechanical properties were increased, and porosity reduced.

3.1.4. Effect of Acid

In classical Bechamp reduction hydrochloric acid is used; for this reason, effect of mineral acid on plaster setting was tested comparing H_3PO_4 and HCl. Acidic solutions increased porosity compared to distilled water, but samples with hydrochloric acid were more dense and compact than those made with phosphoric acid (Table A.4). Presence of mineral acids influenced the gypsum crystallization step, promoting formation of large bulky crystals [24]. Particle size was due to increased growth rate [25]. For hydrochloric acid-containing sample the mechanical strength was increased whereas porosity was similar to samples in absence of acid (Table A.3), However, the goal of our research was to increase plaster permeability and not composite mechanical properties. For

these reasons hydrochloric acid was not used in further experiments. In presence of H_3PO_4 and in absence of carbonate, porosity was higher with respect to samples in Table A.2, indicating that $CaCO_3$ could also act as buffer stopping acid reactivity and controlling porosity.

3.1.5. Permeability Coefficient Measurements

Permeability coefficients were measured for all sample and results reported in Table 1. In order to allow percolation rapidly, porosity obtained only by water evaporation was insufficient to have an acceptable permeability. For samples containing "compact" plaster (series 1 and 3), discharge was very slow and permeability coefficients were estimated from water amount recovered after 24 hours. Using $CaCO_3$ as porogen, plaster permeability increased by three orders of magnitude allowing to run experiments in short times.

In a ^{1}H NMR relaxation study of water, confined in porous medium of hardening gypsum (without porogen), coexistence of two water populations were described in permeable and disordered porous plaster structure. The first population (P1) extended uniformly in space while the second one (P2) was more confined and isolated in some clusters of gypsum needles [20]. Distribution of the two populations was related to water-to-plaster ratio (w/p)
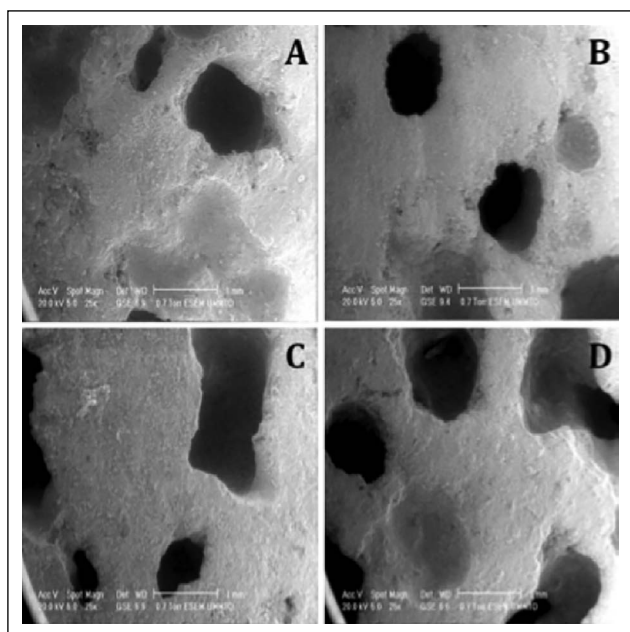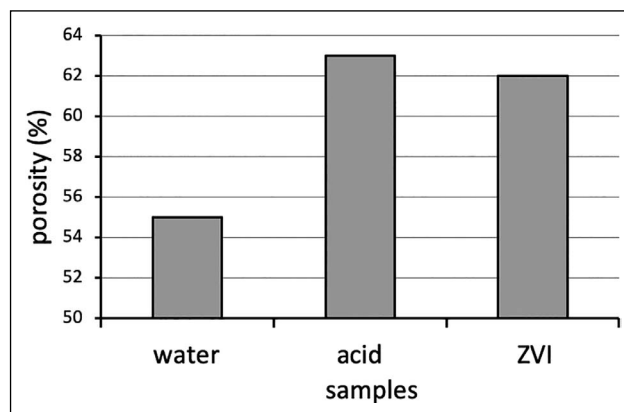
Figure 2. SEM photographs showing a view of porogen-containing hardened gypsum samples, prepared with a water-to-plaster ratio of 0.7, as a function of carbonate amounts (with 1.1 % phosphoric acid, w/w). $CaCO_3$: A=0.2%, B=0.5g, C=0.7g, D= 0.9% (w/w); length scale bar is 1 mm and magnification x25).

values: at low w/p value, P2 increased and P1 decreased, in agreement with total porosity observed as a function of w/p. Moreover, from a micro-structural point of view, an intricate percolation networks of needles with different packing density exists in hardened plaster structure where percolation threshold allowing water exchange was about w/p=0.6. Below w/p=0.6, there was an extremely slow exchange rate (almost zero) and the two water populations were almost independent. Above w/p=0.7, there was a small but finite exchange rate between the two water populations, but composite permeability was not sufficient to run PRB kinetic studies in short times.

Porosity of different plaster slabs, obtained from sample densities, with and without porogen, was not so different (62% vs 55%, Table S2), however permeability was extremely dependent on porogen presence, differing by about three orders of magnitude (Table 1).

Figure 3. Porosity optimization as a function of different components of BRP (water, phosphoric acid and ZVI) plaster (50.0 g, 40.0%); water (56.0%); $CaCO_3$ (0.2%); H_3PO_4 (0.2%).

3.2. Degradation of 4-Nitroaniline
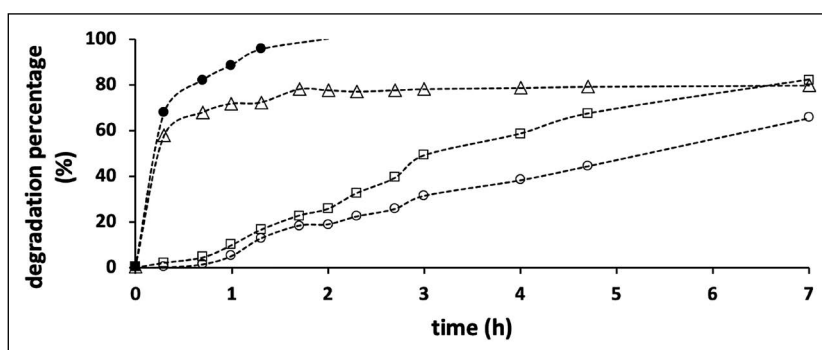#### 3.2.1. *Column Formulation*

Only composites with a permeability allowing the study of PRB chemical reactivity in a one-day period, were used in pollution removal tests.

Figure 3 reported optimization of all composite components (water, calcium carbonate, phosphoric acid, ZVI) for a fixed amount of plaster to improve different physical properties. Composite formulation, used to mold columns, contained plaster and water with 0.7 ratio, 0.2% $CaCO_3$ and 0.4% H_3PO_4 (per 50 g of plaster).

3.2.2. *ZVI Reactivity in Batch*

Bechamp reduction was checked batchwise. Experiments were run as a function of ZVI amount, in absence and in presence of phosphoric acid to activate reduction. "Classical" reduction [6] was run with acetic acid (or hydrochloric acid), which does not form insoluble species after oxidation of ZVI to Fe(II) or Fe(III). Yellow PNA aqueous solutions were expected to fade as a function of time, following reduction to PNA (Fig. A1).

As a function of time, yellow solutions turned pale and were cloudy: also in absence of H_3PO_4, reduction occurred and after 7 hours almost no PNA remained in solution (Fig. 4). As a function of time, protons were consumed in reduction reaction and solution pH increased (Fig. 5).

Table 1. Permeability coefficients of plaster samples as a function of composition. Experimental conditions: plaster (50.0 g, 41.0%); experiments were an average of five samples

Serie	Water/plaster (w/w)	$CaCO_3$+H_3PO_4 (%)	ZVI (%)	pH values	Permeability coefficient (m/s)
1	0.7	–	–	7.1	$\geq 8.23 \cdot 10^{-8}$
2	0.7	0.4	–	7.4	$2.88 \pm 0.13 \cdot 10^{-5}$
3	0.7	–	2	7.1	$\geq 8.23 \cdot 10^{-8}$
4	0.7	0.4	2	7.3	$2.24 \pm 0.74 \cdot 10^{-5}$

Figure 4. Degradation of PNA in Bechamp reduction as a function of time and of ZVI percentage: 1.2 (O); 2.3 (□); 3.4 (△); 1.0% + 1.0% H_3PO_4 (●); [PNA]=30 mg/l.
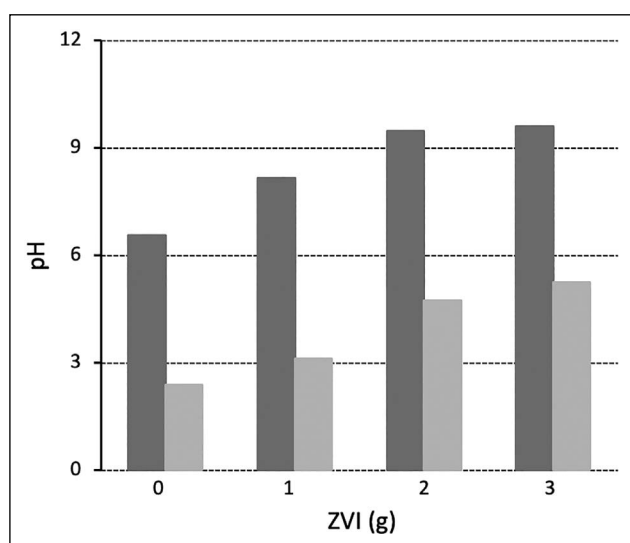

Figure 5. Final pH values of solutions in batch Bechamp reduction after 7 hours, as a function of ZVI: without acid (dark grey); with 1 % H_3PO^4 (light grey).

In presence of H_3PO_4 (0.4%) or higher amount of ZVI (>3%), reaction was faster and total reduction occurred in 1 hour. Solutions were cloudy because of formation of insoluble iron hydroxides or phosphates. Samples recovered after reduction, with or without acid, became violet by standing: redox reaction was not halted to PDA and polymerization of aromatic molecules also occurred, as usual in presence of metal ions [26, 27].

3.2.3. ZVI Reactivity in Column
PNA solutions were added to columns (Fig. 6) and, after percolation, fractions (100 ml) were recovered and analyzed by Vis-UV spectroscopy. In all experiments, yellow color of PNA solutions disappeared indicating that Bechamp reduction occurred in plaster columns. In order to verify chemical effects in colour fading, UV-Vis spectra were registered between 200 and 700 nm: PNA was reduced to PDA indicating that Bechamp reaction occurred in plaster column. As observed in batch experiments, PDA aqueous solutions were not stable as a function of time: pale yellow solutions
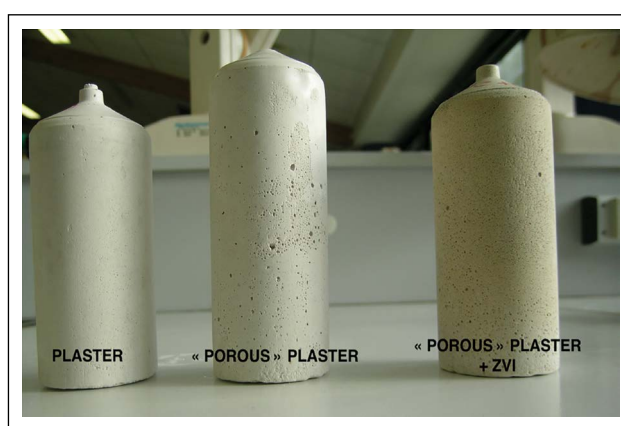
Figure 6. Plaster column composition: plaster (50.0 g, 41.0%); water (57.4%); $CaCO_3$ (0.2%); H_3PO_4 (1.4%); ZVI (2.3%).

became hazy and violet colored, indicating polymerization of aromatic amines.

Degradation profiles, as a function of time at different concentrations of PNA and ZVI, were reported in Figure 7. The flow through the columns was around 0.3 ml/min.

As expected, breakthrough points in the reduction reaction were dependant on ZVI amount included in plaster column; PNA concentration seemed to have less influence because degradation profiles in Figure 7 (except those with low quantity of ZVI) were almost superimposable.

In degradation reaction, PNA amount reduced to PDA by ZVI (in 2.3 and 3.4% experiments) was estimated: e.g. 1.6 L of aqueous PNA solution at 100 mg/L were treated by 3 g of ZVI, meaning a complete inactivation at around 55 mg of PNA per gram of ZVI, or about 2.2×10^{-2} mol PNA per 1 mol Fe(0).

3.3. Analysis After Remediation
Plaster columns and solutions recovered were analyzed at the end of remediation process in order to elucidate the role and reactivity of ZVI trapped in solid.

3.3.1. Solution Analysis
Because of the presence of colored species (PNA and
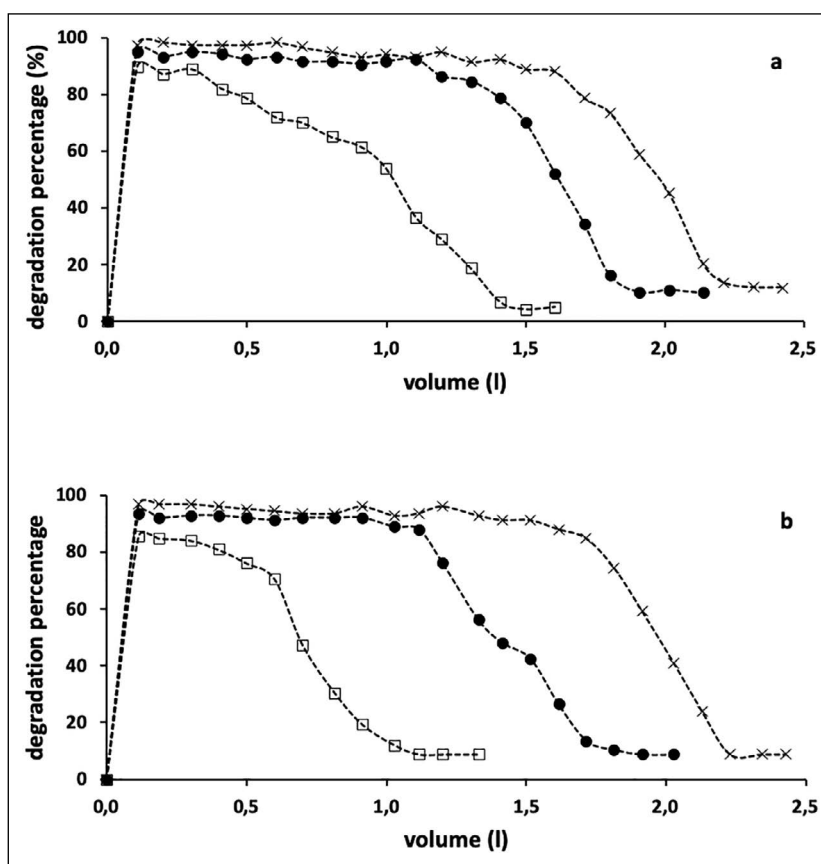
Figure 7. Degradation profiles of p-nitroaniline as percentage (PNA=30 mg/L **(a)**, 100 mg/L **(b)**) as a function of elution volume and ZVI percentage. ZVI: 1.2 (□), 2.3 (●), 3.4 % (X); column composition (without ZVI): plaster (200.0 g, 41.0%); water (57.4%); $CaCO_3$ (0.2%); H_3PO_4 (1.4%).

PDA), a colorimetric analysis of the solutions in order to follow the fate of ZVI, was not possible. However, this analysis was possible in ZVI composite before any reaction. Samples were soaked in distilled water and pH was measured as a function of time. KSCN and o-phenathroline in aqueous solution were used to check presence of Fe(II) or Fe(III) species, respectively. Because of the low amount of iron ionic species in solution, reagents were used in strong excess for ion identification. Presence of Fe(II) was detected in plaster columns (Table A.5) following the reaction between ZVI and phosphoric acid, whereas Fe(III) was not found by colorimetric method.

In ZVI-containing column, during addition of PNA solutions, the first volume eluted was slightly acid (pH=5.22), probably because of traces of phosphoric acid, whereas, later on, pH was determined by the major organic compound present in solution (PDA, pH=8.07; PNA, pH=6.10 for 30 mg/l aqueous solutions).

3.3.2. Solid Analysis

At the end of reduction process, reddish colour of column indicated presence of Fe_3O_4 species, formed because of instability of Fe(II) species in aqueous solution in presence of dioxygen,

XRD diffractograms for plaster samples (Fig. 8) were compatible with those of gypsum (COD 2300259). Typical diffraction angle at 44.8° (2θ) for Fe(0) [28] was not detected by XRD, because in these experimental conditions, iron metal, dispersed in a gypsum matrix, could be observed only at high percentage (>50%). However, in plaster composites containing Fe(0), a diffraction angle at 39.5° was present but disappeared after PNA reduction (Fig. 8).

3.3.3. Iron Reactive Species

Bechamp reduction is a stoichiometric reaction, and not a catalytic one, resulting in a series of parallel reactions, with generation of one or more intermediates and byproducts [29]. ZVI is "consumed" in redox system and passivated during flow of aqueous solutions. Noubactep reported to use the lowest possible Fe(0) loading (e.g. <5 g/l) and work at low temperature (e.g. 15°C) [30]. In an environmental application, it would be possible to alternate in PRB porous plaster blocks (in order to absorb more polluted solution) and ZVI-containing compact plaster blocks (in order to act as reducing agent) to increase the residence time. However, Bechamp reaction in PRB seems to be more complex than in solution. In fact, reduction by Fe(0) occured and contributed significantly to contaminant removal, but the
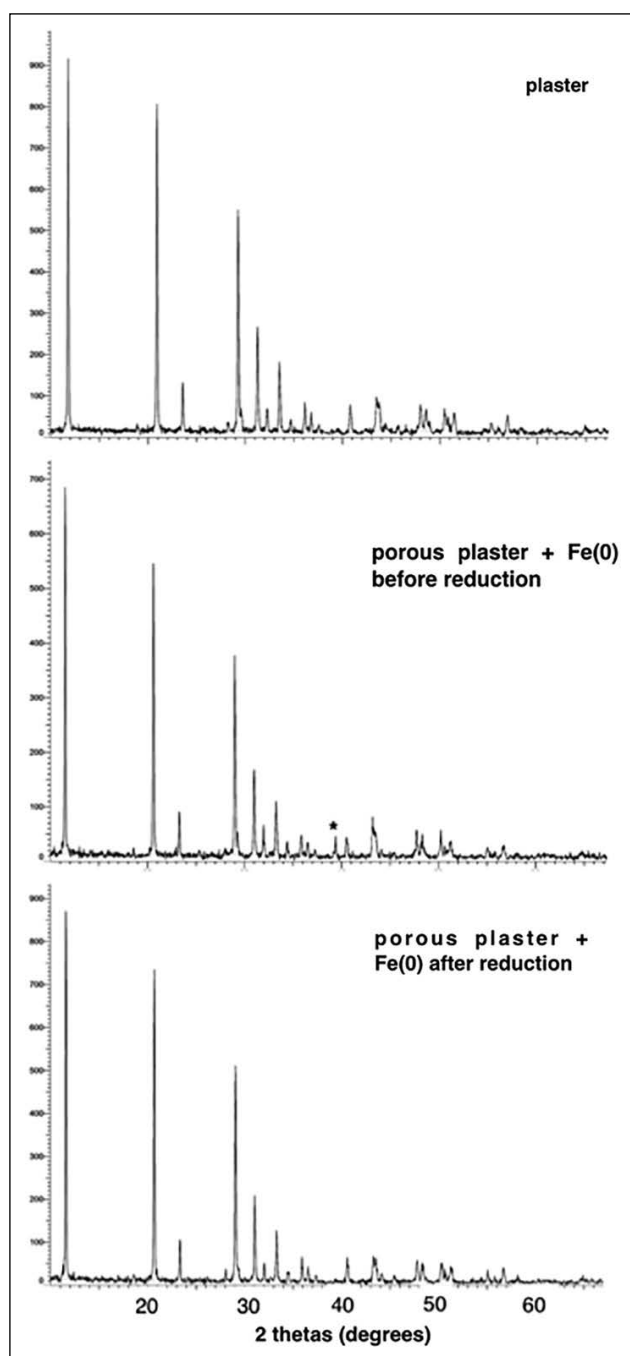
Figure 8. DRX of plaster composites, plaster, plaster + Fe(0) before reduction, and plaster + Fe(0) after reduction. Composites were formulated as in Tables S1 and S4.

mechanism remained unclear. It is matter of debate in ZVI depolluting systems, if, between the Fe(II)/Fe(0) or Fe(III)/Fe(II) couples, which one is involved in the redox reactions [31]. In batch experiments, PNA reduction occurred also without acid suggesting that Fe(0) would be directly involved in redox system; however kinetics, in batch and in column, were not the same (in column the reaction was instantaneous) suggesting that preliminary treatment with

phosphoric acid acted also on ZVI surface, partially generating Fe(II) species. It means that Fe(II) species could be involved in order to accelerate reduction rate, but remains the question of Fe(II) species stability in presence of dioxygen.

In ZVI reactions, concomitant precipitation of iron hydroxydes absorbing organic compounds has been also suggested [32]. From our experience in pollutant co-precipitation methods [33], we cannot totally reject this mechanism [34], but recovering PDA in solution strongly suggested that redox mechanism was predominant.

Finally, we observed that, as a function of time, downflow through the column increased by 25% indicating that plaster columns were embrittled: columns were sensitive to percolation because of calcium sulfate solubility in water and because iron corrosion products formed in situ were partially disrupting their structure.

3.4. Environmental Impact and Cost
An ideal PRB should present the following advantages [35]:
*   stability during PRB lifetime in order to minimize lost of efficiency: Plaster of Paris containing zero valent iron particles: is a stable composite
*   chemical reactivity, which is related to reactant contact time, depending on flow rate and amount of reactant: ZVI is still actif when included in plaster.
*   hydraulic and mechanical performances: PRB permeability has to be higher than aquifer flow in order to not disturb underground flow and not induce polluted flow out of barrier. The supporting material should also be shaped in blocks in order to easily build PRB. Permeability, mechanical properties and shapes of plaster-based PRB can be modulated in formulation step.
*   reduced environmental impact in order to avoid pollution effects. PBR has to be mainly constituted by inert and non-toxic materials, producing non-toxic and harmless by-products: if the main problem in using calcium sulfate-based PRB for geological applications is their relative solubility in water, however they will break up with time discharging in environment no toxic species.
*   cost of PRB building (in terms of materials and construction process) as low as possible in order to be economically feasible: the cost of plaster-based PRB is estimated to be very low and convenient.

Finally, efficiency of ZVI in plaster based-columns suggests use of these composite as precast plaster wall blocks in environmental applications.

4. CONCLUSION

Plaster PRB was used to purify water from soluble organic contaminants, such as 4-nitroaniline. Plaster is one of the most used materials in construction industry. It can be used in PRB and it can incorporate many types of addi-

tives. We have included ZVI to make a reactive component with capacity to remove nitro compounds while the water flow passes through plaster. Use of ZVI as additive in PRB allows removing toxic organic compounds by reduction of nitro function to amino functions. To provide PRB with good flow through properties, formulation of porous plaster with increased porosity was made possible by reaction of calcium carbonate with a small amount of phosphoric acid, which causes evolution of carbon dioxide gas simultaneously with precipitation of calcium phosphate, effectively making plaster less water soluble. Thus improved plaster-based PRB, defining porosity and ZVI particles, can be developed for use in removal of organic compounds from water. This opens possibilities for use of plaster-based PRB in many pollution control technologies where it could be scaled up.

DATA AVAILABILITY STATEMENT

The authors confirm that the data that supports the findings of this study are available within the article. Raw data that support the finding of this study are available from the corresponding author, upon reasonable request.

CONFLICT OF INTEREST

The authors declare that they have no conflict of interest.

FINANCIAL DISCLOSURE

The authors declared that this study has received no financial support.

PEER-REVIEW

Externally peer-reviewed.

REFERENCES

[1] Henderson, A.D., & Demond A.H. (2007). Long-term performance of zero-valent iron permeable reactive barriers: a critical review. *Environmental Engineering Science*, 24, 401–423. [CrossRef]

[2] Grajales-Mesa S.J., & Malina G. (2016). Screening reactive materials for a permeable barrier to treat TCE-contaminated groundwater: laboratory studies. *Environmental Earth Science*, 75, 772–785. [CrossRef]

[3] Dorathi P.J., & Kandasamy P. (2012). Dechlorination of chlorophenols by zero valent iron impregnated silica. *Journal of Environmental Science*, 24, 765–773. [CrossRef]

[4] Zingaretti D., I.Verginelli, Luisetto I., & Baciocchi R. (2020). Horizontal permeable reactive barriers with zero-valent iron for preventing upward diffusion of chlorinated solvent vapors in the unsaturated zone. *Journal of Contaminant Hydrology*, 234, Article 103687. [CrossRef]

[5] Bortone I., Erto A., Di Nardo A., Santonastaso G.F., Chianese S., & Musmarra D. (2020). Pump-and-treat configurations with vertical and horizontal wells to remediate an aquifer. *Journal of Contaminant Hydrology*, 235, Article 103725. [CrossRef]

[6] Béchamp A. (1854). De l'action des protosels de fer sur la nitronaphtaline et la nitrobenzine. nouvelle méthode de formation des bases organiques artificielles de Zinin. *Annales de Chimie et de Physique*, 42, 186–196.

[7] Schabel T., Belger C., & Plietker B. (2013). A mild chemoselective ru-catalyzed reduction of alkynes, ketones, and nitro compounds. *Organic Letters*,15, 2858–2861.

[8] Farooqi Z.H., Khalid R., Begum R., Farooq U., Wu Q., Wu W., Ajmal M., Irfan A., & Naseem K. (2018). Facile synthesis of silver nanoparticles in a cross-linked polymeric system by in situ reduction method for catalytic reduction of 4-nitroaniline. *Environmental Technology*, 40, 1–30. [CrossRef]

[9] Hu R., Cui X., Gwenzi W., Wu S., & Noubactep C. (2018). Fe0/H2O Systems for environmental remediation: the scientific history and future research directions. *Water*, 10(12), 1739–1755. [CrossRef]

[10] Eljamal O., Thompson I.P., Maamoun I., Shubair T., Eljamal K., Lueangwattanapong K., & Sugihara Y. (2020). Investigating the design parameters for a permeable reactive barrier consisting of nanoscale zero-valent iron and bimetallic iron/copper for phosphate removal. *Journal of Molecular Liquids*, 299, Article 112144. [CrossRef]

[11] Maamoun I., Eljamal O., Eljamal R., Falyouna O., & Sugihara Y. (2020). Promoting aqueous and transport characteristics of highly reactive nanoscale zero valent iron via different layered hydroxide coatings. *Applied Surface Science*, 506, Article 145018.

[12] Wantanaphong J., Mooney S.J., & Bailey E.H. (2006). Quantification of pore clogging characteristics in potential permeable reactive barrier (PRB) substrates using image analysis. *Journal of Contaminant Hydrology*, 8, 299–320. [CrossRef]

[13] Touze S., Chartier R., & Gaboriau H. (2004). Etat de l'art sur les barrières perméables réactives (BPR): Réalisations, expériences, critères décisionnels et perspectives; BRGM Orléans, France.

[14] Saadaoui E., Ghazela N., Ben Romdhanea C., & Massoudi N. (2017). Phosphogypsum: potential uses and problems - a review. *International Journal of Environmental Study*, 74, 558–567. [CrossRef]

[15] Chernysh Y., Yakhnenko O., Chubur V., & Roubik H. (2021). Phosphogypsum recycling: a review of environmental issues, current trends and prospects. *Applied Science*, 11, 1575. [CrossRef]

[16] Rumble J., (Ed.). (2019). *CRC handbook of chemistry and physics* (100th ed.). CRC Press.

[17] Lewry A.J., & Williamson J. (1994). The setting of gypsum plaster: part I. The hydration of calcium sulphate hemihydrate. *Journal of Materials Science*, 29, 5279–5284. [CrossRef]

[18] Adrien J., Meille S., Tadier S., Maire E., & Sasaki L. (2016). In-situ X-ray tomographic monitoring of gypsum plaster setting. *Cement and Concrete Research*, 82, 107–116. [CrossRef]

[19] Diaga Seck M., Van Landeghem M., Faure P., Rodts S., Combes R., Cavalie P., Keita E., & Coussot P. (2015). The mechanisms of plaster drying. *Journal of Materials Science*, 50, 2491–2501. [CrossRef]

[20] Jaffel H., Korb J.P., Ndobo-Epoy J.P., Morin V., & Guicquero J.P. (2006). Probing Microstructure Evolution during the Hardening of Gypsum by Proton NMR Relaxometry. *The Journal of Physical Chemistry B*, 110, 7385–7391. [CrossRef]

[21] Fisher R.D., Hanna J.V., Reesc G.J., & Walton R.I. (2012). Calcium sulfate-phosphate composites with enhanced water resistance. *Journal of Materials Chemistry*, 22, 4837–4846. [CrossRef]

[22] Pham Minh D., Dung Tran N., Nzihou A., & Sharrock P. (2014). Novel one-step synthesis and characterization of bone-like carbonated apatite from calcium carbonate, calcium hydroxide and orthophosphoric acid as economical starting materials. *Materials Research Bulletin*, 51, 236–243. [CrossRef]

[23] Lanzóna M., & García-Ruiz P.A. (2012). Effect of citric acid on setting inhibition and mechanical properties of gypsum building plasters. *Construction and Building Materials*, 28, 506–511. [CrossRef]

[24] Mori T. (1982). The effect of boric acid on the thermal behavior of cast gypsum. *Dental Materials Journal*, 1, 73-80. [CrossRef]

[25] Al-Othman A., & Demopoulos G.P. (2009). Gypsum crystallization and hydrochloric acid regeneration by reaction of calcium chloride solution with sulfuric acid. *Hydrometallurgy*, 96, 95–102. [CrossRef]

[26] Lajoie-Halova B., Brumas V., Fiallo M.M.L., & Berthon G. (2006). Copper(II) interactions with non-steroidal anti-inflammatory agents. III – 3-Methoxyanthranilic acid as a potential OH-inactivating ligand: a quantitative investigation of its copper handling role in vivo. *Journal of Inorganic Biochemistry*, 100, 362–373. [CrossRef]

[27] Sapurina I., & Stejskal J. (2008). The mechanism of the oxidative polymerization of aniline and the formation of supramolecular polyaniline structures. *Polymer International*, 57, 1295–1325. [CrossRef]

[28] Khalil A.M.E., Eljamal O., Amen T.W.M., Sugihara Y., & Matsunaga N. (2018). Scrutiny of interference effect of ions and organic matters on water treatment using supported nanoscale zero-valent iron. *Environmental Earth Science*, 77, 489–501. [CrossRef]

[29] Popat V., & Padhiyar N. (2013). Kinetic study of bechamp process for P-Nitrotoluene reduction to P-Toluidine. *International Journal of Chemical Engineering and Applications*, 4(6), 401–405. [CrossRef]

[30] Noubactep C. (2009). An analysis of the evolution of reactive species in Fe0/H2O systems. *Journal of Hazardous Materials*, 168(2-3), 1626–1631. [CrossRef]

[31] Noubactep C. (2008). A Critical Review on the Process of Contaminant Removal in Fe0–H2O Systems. *Environmental Technology* 29(8), 909–920. [CrossRef]

[32] Noubactep C. (2009). Characterizing the discoloration of methylene blue in Fe0/H2O systems. *Journal of Hazardous Materials*, 166(1), 79–87. [CrossRef]

[33] Lemlikchi W., Sharrock P., Fiallo M., Nzihou A., & Mecherri M.O. (2014). Hydroxyapatite and Alizarin sulfonate ARS modeling interactions for textile dyes removal from wastewaters. *Procedia Engineering*, 83, 378–385. [CrossRef]

[34] Noubactep C. (2007). Processes of contaminant removal in "fe0-h2o" systems revisited: the importance of co-precipitation. *Open Environmental Sciences*, 1, 9–13. [CrossRef]

[35] ITRC. (2021 December 15). Technical Regulatory Guidance Document: Permeable Reactive Barrier: Technology Update (PRB-5, 2011). https://connect.itrcweb.org/HigherLogic/System/DownloadDocumentFile.ashx?DocumentFileKey=fd058d3e-9bdc-4103-8f13-4195efa8499f

Appendices

Table A1. Physical and mechanical properties of plaster samples (density, porosity, indirect tensile strength) as a function of plaster/water ratio (w/w); experimental conditions: plaster (50.00 g); measurements were an average from ten samples

Water/plaster ratio (w/w)	Density (g/ml)	Porosity (%)	Indirect tensile strength MPa)
0.5	1.15±0.04	50.46±0.40	7.14±0.43
0.6	1.10±0.04	52.71±0.33	5.47±0.41
0.7	1.04±0.06	55.06±0.61	4.48±0.43
0.8	0.99±0.05	57.39±2.00	3.57±0.19

Table A2. Physical and mechanical properties of plaster samples (density, porosity, indirect tensile strength) as a function of H_3PO_4 added; experimental conditions: plaster (50.0g, 41.0%); water (58.2 %); $CaCO_3$ (0.2%)

H_3PO_4 (g)	H_3PO_4 (%)	Density (g/ml)	Porosity (%)	Indirect tensile strength (MPa)
0	0	1.04±0.06	55.06±0.61	4.48±0.43
0.34	0.3	0.86±0.06	63.08±2.72	1.48±0.09
0.68	0.6	0.76±0.01	66.97±0.35	1.15±0.73
1.01	0.8	0.74±0.03	67.94±2.62	1.04±0.25
1.35	1.1	0.72±0.01	69.13±1.80	0.83±0.08

Table A3. Physical and mechanical properties of plaster samples (density, porosity, indirect tensile strength) as a function of ZVI added; experimental conditions: plaster (50.0 g, 41.0%); water (57.4%); $CaCO_3$ (0.2%); H_3PO_4 (0.2%)An example of a table (9pt)

ZVI (g)	ZVI percentage (%)	Density (g/ml)	Porosity (%)	Indirect tensile strength (kPa)
0	0	0.86±0.06	63.08±2.72	1.48±0.09
1.00	1.2	0.88±0.29	62.19±0.66	1.26±0.27
2.00	2.3	1.17±0.05	49.56±0.37	1.93±0.30
3.00	3.4	1.36±0.05	41.23±0.93	3.18±0.88
5.00	5.6	1.36±0.06	41.32±0.57	3.14±0.51

Table A4. Physical and mechanical properties of plaster samples (density, porosity, indirect tensile strength) as a function of acid added (1.4%); experimental conditions: plaster (50.0 g, 41.6%); water (58.2 %); $CaCO_3$ (0.2%)

Acid	Density (g/ml)	Porosity (%)	Indirect tensile strength (MPa)
0	1.04±0.06	55.06±0.61	4.48±0.43
H_3PO_4	0.52±0.07	77.55±0.61	1.89±0.65
HCl	0.94±0.02	59.48±0.67	5.87±1.90

Table A5. pH values and qualitative colorimetric results for ionic iron species in plaster-based composites soaked in distilled water
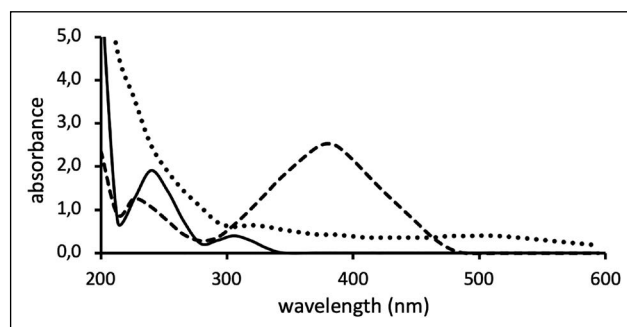
	pH (t=0)	pH (t=48 h)	Fe(II) test	Fe(III) test
Plaster	6.92	6.87	Negative	Negative
Plaster+ZVI	6.76	7.45	Negative	Negative
Plaster+ZVI+$CaCO^3$+H^3PO_4	6.91	7.09	Positive	Negative

Figure A1. (Absorption spectra of PNA (---), PDA (___) and PDA polymerization product (…) in aqueous solutions: [PNA]=[PDA]=30 mg/l; path-length quartz cell=0.2 cm.